Available online at www.sciencedirect.com
ScienceDirect
Applied Catalysis B: Environmental 81 (2008) 267–273
APPLIED CATALYSIS B: ENVIRONMENTAL
www.elsevier.com/locate/apcatb

Preparation of polyaniline-modified TiO_2 nanoparticles and their photocatalytic activity under visible light illumination

Xueyan Li [a,b], Desong Wang [b,*], Guoxiang Cheng [a], Qingzhi Luo [b], Jing An [a,b], Yanhong Wang [b]

[a] College of Material Science and Engineering, Tianjin University, Tianjin 300072, China
[b] College of Science, Hebei University of Science and Technology, Shijiazhuang Hebei 050018, China

Received 4 December 2006; received in revised form 13 December 2007; accepted 16 December 2007
Available online 6 January 2008

Abstract

Titanium dioxide nanoparticles were modified by polyaniline (PANI) using 'in situ' chemical oxidative polymerization method in hydrochloric acid solutions. Powder X-ray diffraction (XRD), transmission electron microscopy (TEM), Fourier-transform infrared spectra (FT-IR), X-ray photoelectron spectroscopy spectrum (XPS) and UV–vis spectra were carried out to characterize the composites with different PANI contents. The photocatalytic degradation of phenol was chosen as a model reaction to evaluate the photocatalytic activities of the modified catalysts. Results show that TiO_2 nanoparticles are deposited by PANI to mitigate TiO_2 particles agglomeration. The modification does not alter the crystalline structure of the TiO_2 nanoparticles according to the X-ray diffraction patterns. UV–vis spectra reveal that PANI-modified TiO_2 composites show stronger absorption than neat TiO_2 under the whole range of visible light. The resulting PANI-modified TiO_2 composites exhibit significantly higher photocatalytic activity than that of neat TiO_2 on degradation of phenol aqueous solution under visible light irradiation ($\lambda \geq 400$ nm). An optimum of the synergetic effect is found for an initial molar ratio of aniline to TiO_2 equal to 1/100.

Keywords: Photocatalytic activity; Titanium dioxide; Phenol degradation; Polyaniline

1. Introduction

Photocatalytic degradation is an efficient and economical method to decompose organic pollutions into less dangerous matter. As a photocatalyst, TiO_2 has the advantages of high chemical stability, high photocatalytic activity to oxidize pollutants in air and water, relative low-price and nontoxicity [1]. However, the wide band gap of TiO_2 (3.2 eV) only allows it to absorb the ultraviolet light (<387 nm) that occupies only a small fraction (3–5%) of the solar photons, which limits its wide use. It is of paramount importance to improve the photocatalytic efficiency of TiO_2 by shifting its optical response from the UV to the visible range without the decrease of photocatalytic activity. In recent years, several groups have reported investigations to convert TiO_2 absorption from the ultraviolet to the visible region by doping TiO_2 with transition metals such as Cr, Mn, Fe, V, etc. [2–6]. Recently, doping TiO_2 with nonmetal atoms has received much attention. For example, the doping of nitrogen [7–9], carbon [10–13], sulfur and iodine [14,15] in TiO_2 can lower its band gap and shift its optical response to the visible light region. In addition, a variety of dyes can be used to photosensitize TiO_2 particles by absorbing visible light photons and inject electrons to conduction band (CB) of TiO_2, so as to improve the efficiency of visible light [16,17].

At present, attention is paid to conducting polymers, which are used as photosensitizers to modify TiO_2 nanoparticles [18]. Conducting polymers have already been widely used in photovoltaic devices such as solar cells, light-emitting diodes and corrosion-protecting paint. Although there are plenty of conducting polymers, little work has been done on using conducting polymer to modify TiO_2 to degrade organic pollutions. As a typical conducting polymer, polyaniline (PANI) has unique electrical, optical and photoelectric properties. And most importantly, it is cheaper than other conducting polymers. Recently, Li reported hybrid

* Corresponding author. Tel.: +86 31188632235; fax: +86 31188623769.
E-mail address: dswang06@126.com (D. Wang).

0926-3373/$ – see front matter © 2007 Elsevier B.V. All rights reserved.
doi:10.1016/j.apcatb.2007.12.022

composites of conductive polyaniline and nanocrystalline TiO_2, which were prepared by self-assembling and graft polymerization [19]. Compared with neat TiO_2 nanoparticles, the nanocomposites showed better photocatalytic activity in photodegradation of methyl orange under sunlight. Zhang has got polyaniline-anatase TiO_2 nanocomposites powders and investigated their solid-phase photocatalytic degradation [20].

In the present study, a series of polyaniline-TiO_2 nanocomposite powders with different PANI/TiO_2 ratios were prepared by 'in situ' chemical oxidative polymerization of aniline. In addition, their photocatalytic degradation of phenol was investigated. Results indicate that the introduction of PANI to TiO_2 nanoparticles can enhance the photocatalytic efficiency of TiO_2 under visible light irradiation.

2. Experimental

2.1. Reagents and materials

Phenol, aniline, ammonium peroxydisulfate and hydrochloric acid were obtained from Tianjin Chemical Reagents Company. All these reagents were of AR grades and used without further purification with the exception of aniline that had been distilled before used.

Nanoparticulate TiO_2, which was mostly anatase, with an average particle size of ca.15 nm and BET specific surface area of ca.70 m^2/g, was prepared by sol–gel hydrolysis and condensation of ethanol solutions of tetrabutyl titanate ($Ti(OC_4H_9)_4$) in our laboratory.

2.2. Synthesis of polyaniline-modified TiO_2

Polyaniline-modified TiO_2 composites were prepared by chemical oxidative polymerization of aniline in the presence of TiO_2 nanoparticles. 2.0 g nanocrystalline TiO_2 particles were dispersed into 80 ml of 1 mol·L^{-1} HCl aqueous solutions with ultrasonic vibrations for 30 min to obtain a uniform suspension. Quantitative aniline was added into this mixture dropwise under vigorously stirring in the ice-water bath, after which ammonium peroxydisulfate (APS) was dissolved in 1 mol·L^{-1} HCl aqueous solutions with the molar ratio of aniline to APS (1:1) was added to the reaction vessel. Then the mixture was allowed to polymerize under stirring for 6 h. Finally the polyaniline-modified TiO_2 nanoparticles were filtered and washed with large amount of deionized water, then with 100 mL of ethanol and 50 mL of ether, after that the nanoparticles were dried at 80 °C till the constant mass was reached. In the experiment, different initial molar ratios of aniline to TiO_2 (from 1/60 to 1/120) were used to obtain TiO_2 nanoparticles deposited by PANI. In this way, a series of PANI/TiO_2 nanocomposites with initial molar ratios of aniline to TiO_2 (1/60, 1/80, 1/100, 1/120) were prepared, being referred to as PANI/$TiO_2$60, PANI/$TiO_2$80, PANI/$TiO_2$100, PANI/$TiO_2$120, respectively. To confirm the effect of PANI in the composites, the neat TiO_2 particles were treated in the same procedure as that of composites except that aniline was not added.

2.3. Characterizations of polyaniline-modified TiO_2

Transmission electron microscopy (TEM) study was carried out on a tecnai G2 F20 electron microscopy instrument, which was equipped with an energy dispersive X-ray (EDX) detector. The samples of TEM were prepared by dispersing the final nanoparticles in ethanol; the suspension was then dropped on carbon-copper grids.

Fourier-transform infrared spectra (FT-IR) of the samples were recorded on spectrometer (SHIMADZU) in the range of 400–4000 cm^{-1}. Measurements were performed in the transmission mode in spectroscopic grade KBr pellets for all the powders.

The composites X-ray diffraction (XRD) patterns were performed in the range of 2θ = 10–90° on a Rigaku D/MAX-2500 diffractometer, using Cu Kα radiation (l = 0.15406 nm) as X-ray source, operated at 40 kV and 100 mA. Crystallite size of anatase TiO_2 can be calculated from the line broadening by Scherrer's formula.

A Varian Cary 100 Scan UV–vis system equipped with an integrating sphere attachment was used to obtain the reflectance spectra of the catalysts over a range of 200–800 nm. Integrating sphere USRS-99-010 was employed as a reflectance standard.

XPS measurements were performed in a Perkin-Elmer PHI1600 ESCA system with an Mg Kα X-ray source. All binding energies were referenced to the C1s peak at 284.8 eV of the surface adventitious carbon.

The degradation of phenol and the intermediate products were identified by HPLC (SHIMADZU LC-10AT) equipped with a SHIMADZU C18 ODS column (4.6 mm × 150 mm, 5 μm). The mobile phase was 15% methanol and 85% water flowing at a rate of 0.8 mL·min^{-1}.

2.4. Photocatalytic activity test

The photocatalytic activities of the samples were evaluated by the degradation of phenol in an aqueous solution. 400 ml phenol aqueous solution with concentration of 50 mg·L^{-1} was mixed with 1 g·L^{-1} catalysts, which was exposed to illumination of tungsten halogen lamp (300 W) with visible light by removing light below than 400 nm using a filter. A circulating water jacket was used to cool the reaction vessel. Before turning on the lamp, the suspension containing phenol and photocatalyst were magnetically stirred in a dark condition for 60 min till an adsorption–desorption equilibrium was established. Samples were then taken out regularly from the reactor and centrifuged immediately for separation of any suspended solid. The transparent solution was analyzed by a 754 UV–vis spectrometer. The concentration of phenol was calculated by a calibration curve. At the end of each photoreactivity experiment, the resulting suspension was centrifugalized, the solution was removed, and the separated catalyst was reused for the further photocatalytic experiment. This process was repeated for five or more times to check the stability of the composite photocatalyst.

3. Results and discussion

3.1. TEM images

The nanoparticles of neat TiO_2 and polyaniline-modified TiO_2 are clearly displayed on their images in Fig. 1. From the TEM images, we find that PANI-modified TiO_2 does not change the size of neat TiO_2 significantly, as shown in Fig. 1(a) and (b). The sizes of both modified and neat TiO_2 are monodisperse about 10–20 nm. Moreover, the crystal lattice line can be clearly found in the TEM images. The aggregations of both kinds of particles are caused by high surface energy; however, the agglomeration of the modified one is alleviated obviously compared with that of the neat. Generally, PANI synthesized by a chemical oxidative method in hydrochloric acid solution is the emeraldine salt (ES) form (Fig. 2), only which is electrically conducting. Anatase TiO_2 nanoparticles were deposited by PANI (ES) so as to avoid TiO_2 particles agglomeration because the positive charges exclude each other.

Result of EDX spectrum shows that in addition to H element, the composite is composed of N, C, O, Ti elements. The content of elements lists in Table 1. The high contents of Ti and N elements confirm that TiO_2 particles are coated by PANI partly. Trace Cl atoms come from dopant hydrochloric acid in the ES (PANI) form. Cu atoms should be the copper grids in the performance of TEM.

3.2. XRD patterns

The XRD patterns of neat TiO_2 and PANI-modified TiO_2 are compared in Fig. 3. In the patterns, anatase diffraction peak at 25.3°, 37.8° and 48.1° appeared, which attributed to the 101, 004, 200 reflections, respectively. This indicates that only anatase phase can be indexed from the patterns, and that the rutile and brookite phases of TiO_2 are not observed. Moreover, polyaniline-modified TiO_2 particles do not cause any change in

Table 1
EDX elemental composition of PANI/TiO_2 composite

Element	C(K)	N(K)	O(K)	Cl(K)	Ti(K)	Cu(K)
Weight%	13.567	7.809	24.577	0.134	46.315	7.595
Atomic%	26.186	12.926	35.612	0.087	22.416	2.771

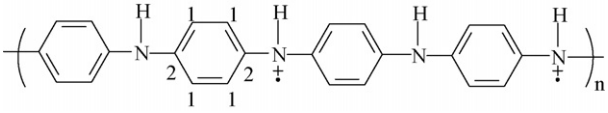

Fig. 2. Structure of emeraldine salt (ES) form of PANI.

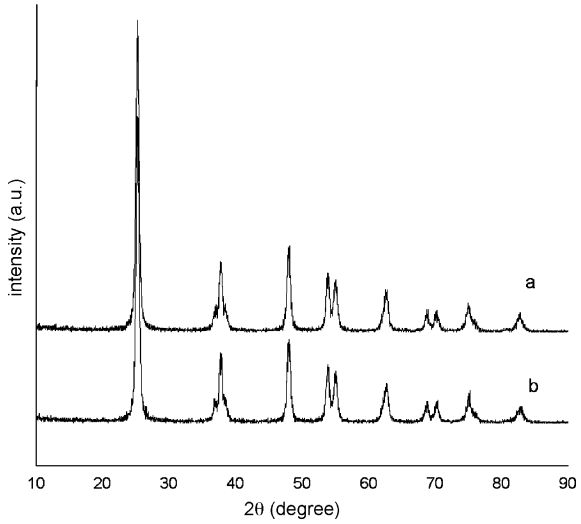

Fig. 3. XRD patterns of (a) neat TiO_2 and (b) PANI modified TiO_2 (PANI/$TiO_2$100).

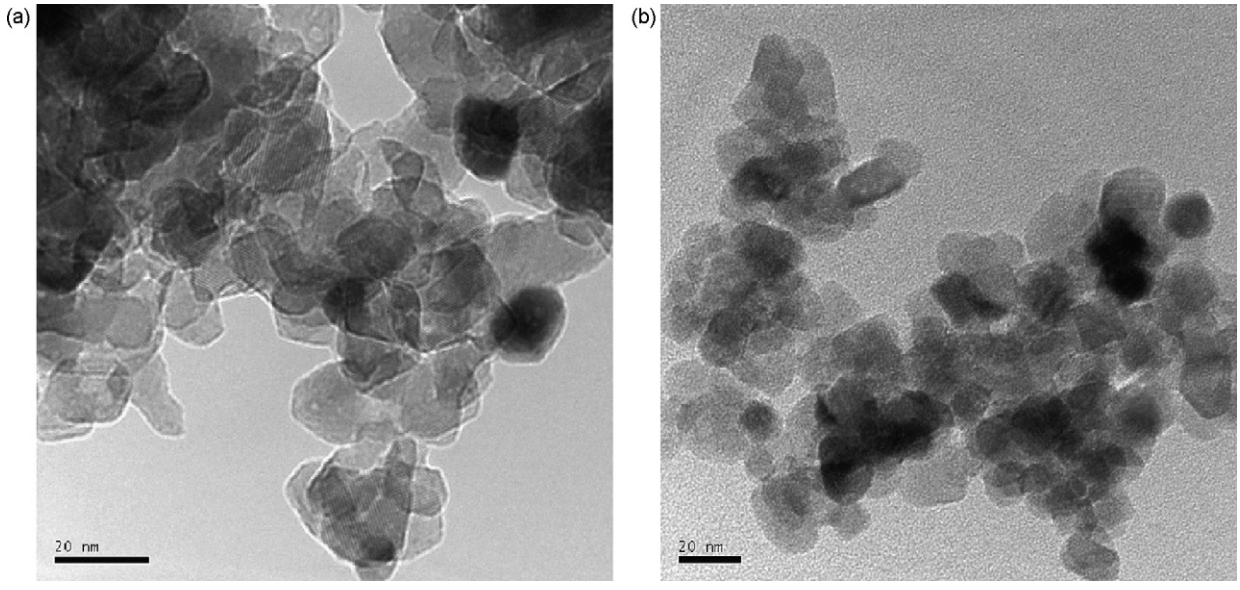

Fig. 1. TEM images of (a) neat TiO_2 and (b) PANI-modified TiO_2 (1/100).

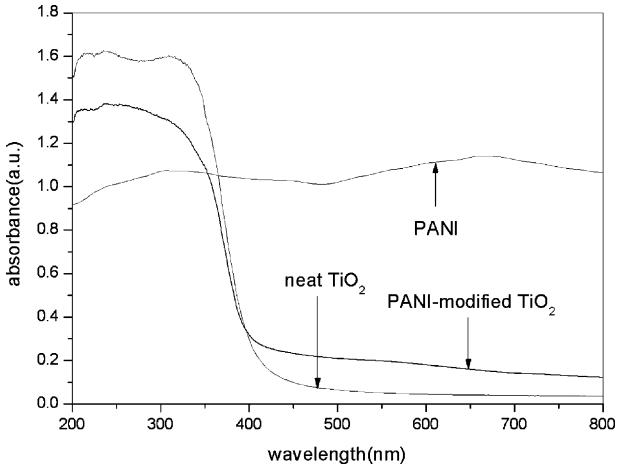

Fig. 4. UV–vis diffuse reflectance spectra of PANI-modified TiO_2, PANI and neat TiO_2.

peak positions and shapes compared with neat TiO_2. This shows that polyaniline-modified TiO_2 particles prepared by 'in situ' polymerization do not change the crystalline structure of neat TiO_2. The main peak of modified catalyst, however, is slightly lower than that of neat TiO_2. It also be should noted that no new diffraction peak appeares in the pattern of PANI-modified TiO_2. This suggests that PANI is amorphous in the composite. The mean size of anatase TiO_2 and modified TiO_2, calculated from Scherrer's formula, are 13.3 and 14 nm, respectively. The results are in accordance with the TEM images.

3.3. UV–vis diffuse reflectance spectra

UV–vis diffuse reflectance spectra of modified sample, PANI and neat TiO_2 are shown in Fig. 4. It is obvious that PANI has high absorption either in the UV range or in the visible light region. Compared with neat TiO_2, the absorption of PANI-modified TiO_2 sample increases over the whole range of visible light whereas decreases in the UV range. This indicates that our method is effective to extend the absorption of TiO_2 to visible light range. The band gap energies (E_g) of modified and neat TiO_2, obtained from the wavelength values corresponding to the intersection point of the vertical and horizontal parts of the spectra using the equation: $hc/\lambda = E_g$, where E_g is the band gap energy (eV), h the Planck's constant, c the light velocity (m/s) and λ the wavelength (nm), are 3.02 and 3.07 eV, respectively. It shows that the band gap energies of the PANI-TiO_2 nanocomposites are lower than that of neat TiO_2 nanoparticles. So the PANI-TiO_2 nanocomposites can be excitated to produce more electron-hole pairs under visible light illumination, which could result in higher photocatalytic activities.

3.4. FT-IR analysis

Fig. 5 compares the FT-IR absorption spectra of neat TiO_2, PANI-HCl and PANI/$TiO_2$100 composite. The main characteristic peaks of doped PANI are assigned as followed [21,22]: the band at 3454 cm^{-1} is attributable to N–H stretching mode, C=N and C=C stretching mode for the quinonoid (Q) and

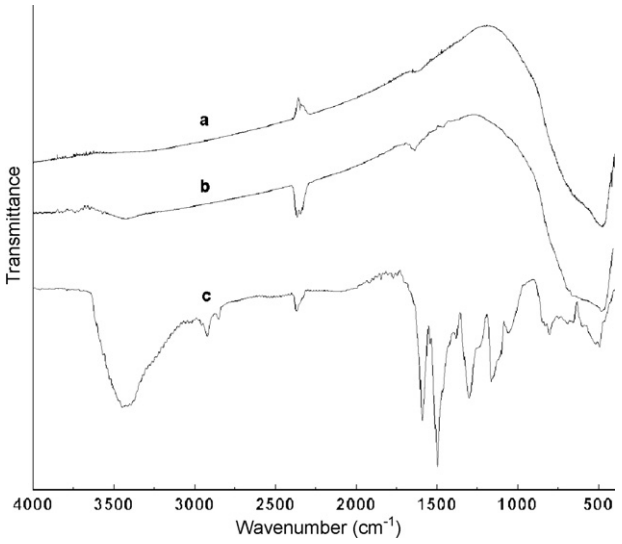

Fig. 5. FT-IR spectra of (a) neat TiO_2, (b) PANI/$TiO_2$100 composite and (c) PANI doped by HCl.

benzenoid (B) rings occur at 1587 and 1492 cm^{-1}. The bands at 1290 and 1226 cm^{-1} have been attributed to C–N stretching mode for benzenoid unit, while the band at 1155 cm^{-1} is assigned to quinonoid unit of doping PANI. The characteristic peak of TiO_2 at 484 cm^{-1} is so wide that it hides the finger peak in the PANI/TiO_2 composite. There is a so small amount of PANI in the composite that only the peaks at 3421 and 1625 cm^{-1} appeared corresponding to the N–H stretching vibration and C=N bond, respectively. Other peaks disappeared in the spectrum of the composite due to the restriction of PANI on TiO_2. Zhang found that there is a strong interaction of H-bonding between PANI and TiO_2 nanoparticles [20]. Low initial concentration of aniline in the polymerization solution results in thinner PANI layer on TiO_2 particles [23].

3.5. XPS analysis

In the X-ray photoelectron spectroscopy spectrum of PANI-modified TiO_2 (shown in Fig. 6), the elements of C, O, Ti and N

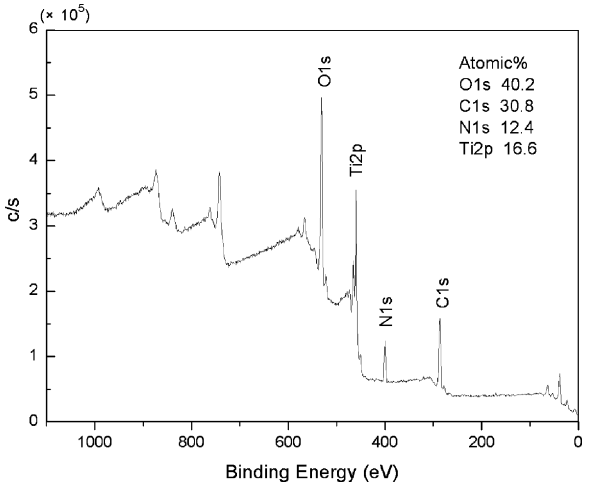

Fig. 6. XPS spectrum of PANI-modified TiO_2.

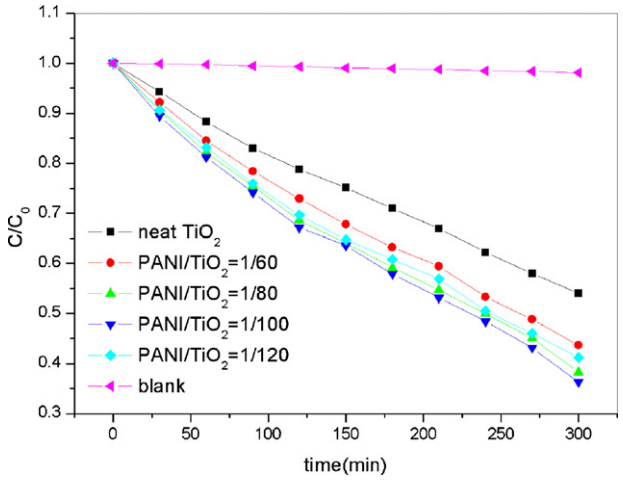

Fig. 7. The photocatalytic degradation of phenol in the presence of neat TiO_2 and modified TiO_2 catalysts with different PANI contents and self-degradation of phenol under visible light illumination.

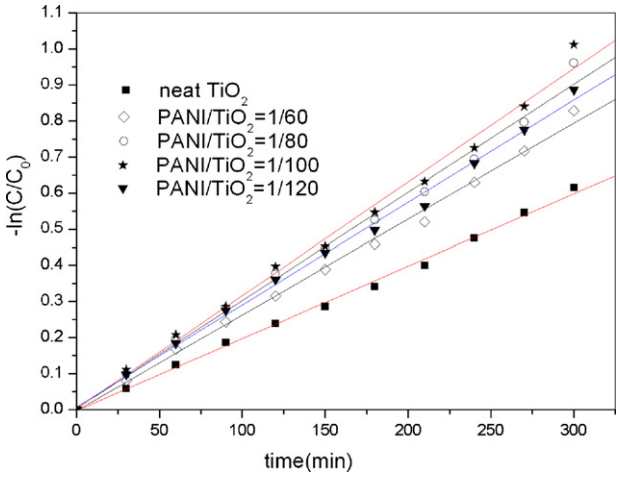

Fig. 8. Apparent first-order linear transforms $-\ln(C/C_0)$ of phenol degradation kinetic plots for neat TiO_2 and modified TiO_2 with different PANI contents under visible light illumination.

can be detected and their binding energies are 284.8, 529.8, 458.5, 400.3 eV, respectively. We also measured C1s and O1s core levels. The results imply that three peaks are observed at binding energies of 284.8, 286.3, 288.6 eV for C1s and two peaks at 529.8, 531.9 eV for O1s. The peak (284.8 eV) of C1s indicates the presence of ^{1}C and the peak (286.3 eV) is attributed to ^{2}C in the structure of PANI (shown in Fig. 2). A small quantity of C atoms whose binding energy is 288.6 eV suggests the presence of C–O–Ti bond [24]. The signal of O1s at 529.8 eV confirms the Ti–O bond in the TiO_2 and the other peak at 531.9 eV is attributed to the presence of H-bonds of TiO_2 and polyaniline. It could be infered that the tight combination of TiO_2 and PANI enhances the photocatalytic activity.

3.6. Photocatalytic activity

Photocatalytic activity tests were investigated by the degradation of phenol in aqueous solution under visible light irradiation. Phenol has a maximum absorption at about 270 nm. Fig. 7 shows the degradation of phenol in aqueous solution in the presence of neat TiO_2, PANI/TiO_2 composites with different initial ratios of aniline to TiO_2 and self-degradation of phenol under visible light irradiation.

The kinetics plots are shown by apparent first-order linear transform $-\ln(C/C_0) = k_{app}t$ in Fig. 8. The self-degradation of phenol is not obvious, which indicates phenol molecule has almost no absorption in visible light range. The activity of neat TiO_2 and modified catalysts can be evaluated by comparing the apparent first-order rate constants (k_{app}) listed in Table 2. Neat TiO_2 and PANI/$TiO_2$100 composite give apparent rate constants of 0.002 min^{-1} and 0.00314 min^{-1}, respectively. The introduction of about 1% PANI to TiO_2 nanoparticles obviously enhanced the photocatalytic activity. It also suggests that the increasing degradation rate of phenol can be seen with the decrease of initial ratio of aniline to TiO_2 from 1/60 to 1/100. When the initial ratios of aniline to TiO_2 lower than 1/100, the degradation rate of phenol begins to decrease.

The basic mechanism of photocatalysis over illuminated TiO_2 was well established [25]. TiO_2 nanoparticles are irradiated with UV light to generate electron-hole pairs, which can react with water to yield hydroxyl and super-oxide radicals to oxidize and mineralize the organic and inorganic molecules. However, the band gap of TiO_2 is 3.2 eV, only UV light can excitate the TiO_2 nanoparticles to generate electrone-hole pairs. Energy of UV light is so little in the solar photons (only 3–5%) that poor photocatalytic efficiency presents under sunlight. One solution to overcome this shortcoming is to use a dye with narrow band gap as a sensitizer, so as to enhance the photocatalytic efficiency of TiO_2. PANI has a band gap of 2.8 eV, which is narrower than 3.2 eV of TiO_2, showing strong absorption in the region of visible light. Hence, it may function as a photosensitizer to TiO_2 [26].

When PANI/TiO_2 nanocomposites are illuminated under visible light, both TiO_2 and PANI absorb the photons at their interface, and then charge separation occurs at the interface. This is because the conduction band of TiO_2 and the lowest unoccupied molecular orbital level of the PANI are well matched for the charge transfer [20]. The electrons generated by conducting PANI can be transferred to the conduction band of TiO_2, enhancing the charge separation and in turn promoting the photocatalytic ability of the photocatalyst.

The synergetic effect between TiO_2 and PANI on the photocatalytic degradation of phenol exists clearly for all the composites. An optimum of the synergetic effect is found for PANI/$TiO_2$100. The mechanism of PANI on the activity of the

Table 2
Appear rate constants (k_{app}) of phenol photodecomposition and linear regression coefficients from a plot of $-\ln(C/C_0) = k_{app}t$

Catalysts	R^2	k_{app} (min^{-1})
Neat TiO_2	0.997	0.002
PANI/$TiO_2$60	0.996	0.00267
PANI/$TiO_2$80	0.993	0.00299
PANI/$TiO_2$100	0.992	0.00314
PANI/$TiO_2$120	0.996	0.00283

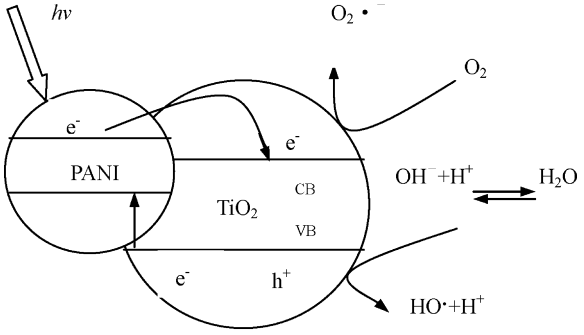

Scheme 1. Mechanism of PANI-modified TiO_2 nanoparticles to enhance photocatalytic activity under visible light irradiation.

composites can be explained by their action as photosensitizer (Scheme 1). Doped PANI as semiconductive material can absorb the visible light irradiation and transfer the photo-generated electron (e^-) into the conduction band of the TiO_2 particles efficiently. Simultaneously, a positive charged hole (h^+) might be formed by electron migrating from TiO_2 valence band to PANI. This electron transfer between PANI and TiO_2 semiconductor and the enhanced photocatalytic activity of the composites was also experimentally observed in some other systems. With this understanding, the role played by PANI can be illustrated by injecting electrons into TiO_2 conduction band under visible light illumination and triggering the formation of very reactive radicals super-oxide radial ion $O_2^{\bullet -}$ and hydroxyl radical $HO^{\bullet}$, which are responsible for the degradation of the organic compound.

$$\mathrm{PANI/TiO_2} + h\nu \rightarrow \mathrm{PANI^+/TiO_2} + \mathrm{e_{CB}^-} \quad (1)$$

$$\mathrm{e_{CB}^-} + \mathrm{O_2} \rightarrow \mathrm{O_2^{\bullet -}} \quad (2)$$

$$\mathrm{PANI^+/TiO_2} \rightarrow \mathrm{PANI/TiO_2} + h_{\mathrm{VB}}^+ \quad (3)$$

$$h_{\mathrm{VB}}^+ + (\mathrm{H_2O} \rightleftarrows \mathrm{H^+} + \mathrm{OH^-}) \rightarrow \mathrm{H^+} + \mathrm{OH^{\bullet}} \quad (4)$$

3.7. Intermediates analysis of phenol degradation process

Using HPLC, intermediate products of phenol degradation were identified. Results indicate that two kinds of intermediate, aromatic and aliphatic compounds are detected as reported in literatures [27,28]. The aromatic intermediates mainly include catechol, hydroquinone and benzoquinon. The aliphatic acids are also detected under this condition in the experiment. It is found that the concentration of phonel is decreased and the concentrations of intermediates are increased during the phenol degradation experiment. Phenol is completely degraded to CO_2 and H_2O at the end of the catalytic experiments.

3.8. Stability of composite photocatalyst

Some kinds of experiments were carried out to confirm the photostability of polyaniline modified TiO_2 photocatalysts. The FT-IR spectra of PANI-modified TiO_2 particles before and after reaction were recorded as shown in Fig. 9. It is found that the shape of composite IR spectrum after photocatalytic

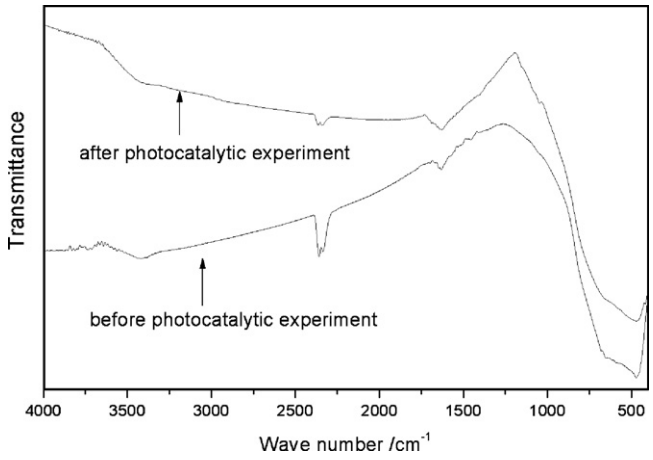

Fig. 9. FT-IR spectra of PANI-modified TiO_2 particles before and after photocatalytic reaction.

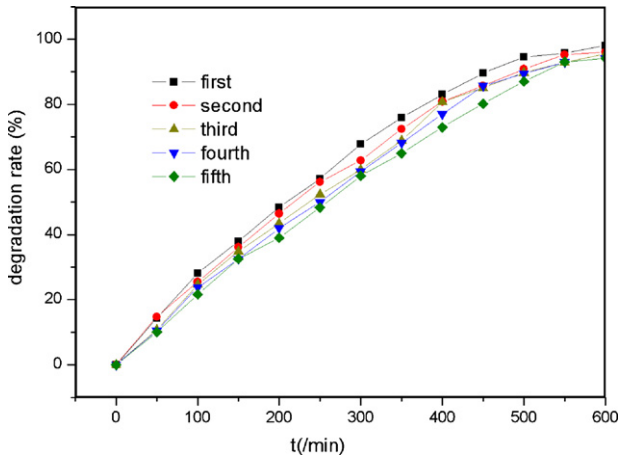

Fig. 10. The photocatalytic experiments of PANI-modified TiO_2 for five cycles.

experiment is similar to that of particles before experiment. It indicates that the structure of PANI-modified TiO_2 does not change during the photo catalytic process. The PANI is very stable and is not chemically transformed to other organic compounds.

It has been confirmed that the PANI-modified TiO_2 shows good stability under irradiation conditions and they continue to maintain perfect photocatalytic activity also after several cycles (Fig. 10). A slight decrease of photoactivity after each cycle is due to slight aggregation of nanoparticles during the catalytic process.

4. Conclusion

PANI-modified TiO_2 composites were prepared by 'in situ' chemical oxidative polymerization of aniline in the TiO_2 suspension. As a photosensitizer to TiO_2, PANI can improve the photocatalytic efficiency of nano-TiO_2 catalyst. The degradation of phenol in an aqueous solution under visible light was carried out to evaluate the photocatalytic activity. It is found that PANI-modified TiO_2 shows significantly higher photocatalytic activity than neat TiO_2 under visible light

illumination. The PANI-modified TiO_2 particulates have good photo stability and perfect photocatalytic activity and the photocatalyst can be recycled five times without significant loss of activity. The size and shape of neat TiO_2 and PANI-modified TiO_2 are presented by TEM images and XRD patterns. UV–vis diffuse reflectance spectra confirmed that the modified catalyst absorbed more photons under visible light irradiation. XPS and FT-IR analysis suggest that there are PANI and TiO_2 in the composites.

References

[1] A. Fujishima, K. Honda, Nature 37 (1972) 238–250.
[2] S.Q. Peng, Y.X. Li, F.Y. Jiang, G.X. Lu, S.B. Li, Chem. Phys. Lett. 398 (2004) 235–239.
[3] J.F. Zhu, Z.G. Deng, F. Chen, J.L. Zhang, H.J. Chen, M. Anpo, J.Z. Huang, L.Z. Zhang, Appl. Catal. B: Environ. 62 (2006) 329–335.
[4] A.G. Rincón, C. Pulgarin, Appl. Catal. B: Environ. 63 (2006) 222–231.
[5] D. Dvoranova, V. Brezova, M. Mazur, M. Malati, Appl. Catal. B: Environ. 37 (2002) 91–105.
[6] X.W. Zhang, M.H. Zhou, L.C. Lei, Catal. Commun. 7 (2006) 427–431.
[7] R. Asahi, T. Morikawa, T. Ohwaki, K. Aoki, Y. Taga, Science 293 (2001) 269–271.
[8] R. Silveyra, L.D.L.T. Sáenz, W.A. Flores, V.C. Martínez, A.A. Elguézabal, Catal. Today 107–108 (2005) 602–605.
[9] Y. Nosaka, M. Matsushita, J. Nishino, A.Y. Nosaka, Sci. Tech. Adv. Mater. 6 (2005) 143–148.
[10] C.K. Xu, R. Killmeyer, M.L. Gray, S.U.M. Khan, Appl. Catal. B: Environ. 64 (2006) 312–317.
[11] M. Janus, B. Tryba, M. Inagaki, A.W. Morawski, Appl. Catal. B: Environ. 52 (2004) 61–67.
[12] W.D. Wang, P. Serp, P. Kalck, J.L. Faria, J. Mol. Catal. A: Chem. 235 (2005) 194–199.
[13] W.D. Wang, P. Serp, P. Kalck, J.L. Faria, Appl. Catal. B: Environ. 56 (2005) 305–312.
[14] A. Koca, M. Sahin, Int. J. Hydrogen Energy 27 (2002) 363–367.
[15] R. Abe, K. Sayama, K. Domen, H. Arakawa, Chem. Phys. Lett. 344 (2001) 339–344.
[16] V. iliev, D. Tomova, L. Bilyarska, L. Prahov, L. Petrov, J. Photochem. Photobio. A: Chem. 159 (2003) 281–287.
[17] H.M. Ding, H. Sun, Y.K. Shan, J. Photochem. Photobio. A: Chem. 169 (2005) 101–107.
[18] L. Song, R.L. Qiu, Y.Q. Mo, D.D. Zhang, H. Wei, Y. Xiong, Catal. Commun. 8 (2007) 429–433.
[19] J. Li, L.H. Zhu, Y.H. Wu, Y. Harima, A.Q. Zhang, H.Q. Tang, Polymer 47 (2006) 7361–7367.
[20] L.X. Zhang, P. Liu, Z.X. Su, Polym. Degrad. Stab. 91 (2006) 2213–2219.
[21] X.W. Li, G.C. Wang, D.M. Lu, Appl. Surf. Sci. 229 (2004) 395–401.
[22] O.P. Dimitrev, Macromolecules 37 (2004) 3388–3395.
[23] S. Irmak, E. Kusvuran, O. Erbatur, Appl. Catal. B: Environ. 54 (2004) 85–91.
[24] B.T. Su, X.H. Liu, X.X. Peng, T. Xiao, Z.X. Su, Mater. Sci. Eng. A: Struct. 349 (2003) 59–62.
[25] G.K.R. Senadeera, T. Kitamura, Y. Wadab, S. Yanagida, J. Photochem. Photobio. A: Chem. 164 (2004) 61–66.
[26] S.X. Xiong, Q. Wang, H.S. Xia, Synth. Met. 146 (2004) 37–42.
[27] N. Wang, Z. Chen, L. Zhu, X. Jiang, B. Lv, H. Tang, J. Photochem. Photobio. A: Chem. 191 (2007) 193–200.
[28] B. Tryba, A.W. Morawski, M. Inagaki, M. Toyada, Appl. Catal. B: Environ. 65 (2006) 86–92.